Hydraulic fracture energy considerations: a 3D numerical simulation compared to microseismic imaging

Neda Boroumand* and Dave Eaton, University of Calgary, Calgary, Alberta
Neda.boroumand@ucalgary.ca

Summary

Hydraulic fracture creation, in unconventional resources, is essential for optimizing hydrocarbon recovery. Microseismic events are mainly small shear failures that occur adjacent to the hydraulic fracture as it propagates and destabilizes the reservoir. When these microseismic events are recorded and mapped, measurements of the hydraulic fracture dimensions in time are possible. With knowledge of reservoir parameters such as: in-situ stress, barrier layer stress contrasts, payzone and layered elastic and material properties and location of layered interfaces, the fracture geometry can also be modeled.

We have developed a numerical algorithm that simulates three-dimensional fracture growth using these input parameters along with the concept of energy balance. Our work is based on Advani's (1990) approach that uses a symmetric three-layered homogeneous geologic model. The fracture is assumed to be a single planar elliptical tensile (Model I) crack that experiences several episodes of energy loss and transformation during propagation. Though many forms of energy losses occur during the hydraulic fracturing process, the ones mainly associated with tensile failure are considered: potential energy, the energy applied to open the fracture; strain energy, the energy used to deform the formation; and surface energy, the energy required to create a new fracture surface.

The modeled fracture length, width, height and effective crack opening pressure are solved at different injection times. The calculated dimensions are compared to the mapped microseismic geometries and effective borehole treatment pressure. By sequentially adjusting the input parameters and comparing the model response to the microseismic image, we determine their influence on the resulting fracture geometry and pressure profile. This shows that energy considerations can serve as a practical method for determining fracture geometry.

Introduction

Energy considerations using a Lagrangian formulation applied to hydraulic fracture propagation was introduced by Biot. et al. (1986) for a propagating two-dimensional (2D) circular crack. Perkins and Krech (1968) derived an energy balance equation using a comparison between laboratory and modeled data. Their energy balance criterion showed that, upon crack extension, when sufficient pressure is supplied to the system to cause formation strain, enough energy needs to be available to create the new fracture surface. Shlyapobersky's (1985) energy analysis of hydraulic fracturing incorporated fracture toughness effects, also known as the "stress-intensity factor". He used this to describe the intensity of the stress concentrated at the crack tip and incorporate it into the surface energy considerations. He also considered the viscous dissipation energy term. In the 1980's, high-viscosity fluids were relied upon mainly to create adequate width and maximize proppant transport. However, in more recent years, depending on the formation and objective, low viscosity fluids (e.g. plain water) have become more prevalent. This is partly due to cost, but also because adequate production rates are achieved (EPA, 2004). Since the example considered in this study uses fresh water as the fracturing fluid, the dissipation energy term is neglected due to assumptions in the fluid consistency and flow behavior index.

Advani et al. (1990) presented the energy balance concept for the purpose of predicting fracture configuration, thus optimizing the hydraulic fracture design. They examined the role of fluid behavior, reservoir and stress properties on the evolution of fracture geometry by evaluating propagation in an isotropic three-layered symmetric model.

In these previous studies however, microseismic data was not readily available. Consequently, validation of previous results was undertaken in other ways such as comparison between results obtained by other models, running injection tests in the field and in the laboratory (while accounting for scale effects) and, in rare cases, observations made in mineback experiments (Warpinski & Tuefel, 1984). Within the petroleum industry, there has been significant progress in understanding the hydraulic fracturing process in order to reduce cost and optimize production. The addition of microseismic imaging has provided additional insights.

Method

The energy balance formulation to simulate elliptical fracture growth uses the following generic formulation,

$$U_p = U_s + U_f + Q, \tag{1}$$

where U_p is the energy required to open the fracture using an effective pressure, U_s is the energy corresponding to the crack opening width, U_f is the Griffith fracture surface energy for crack propagation (Lee et al., 1991). The final term, Q, contains all other forms of energy losses (i.e. thermal, hydrostatic and fluid dissipation ($\dot{D}$), etc.). Figure 1 shows the different energy contributions of the hydraulic fracture in a simple three-layered symmetric formation, surrounded by microseismic activity indicating fracture extension.

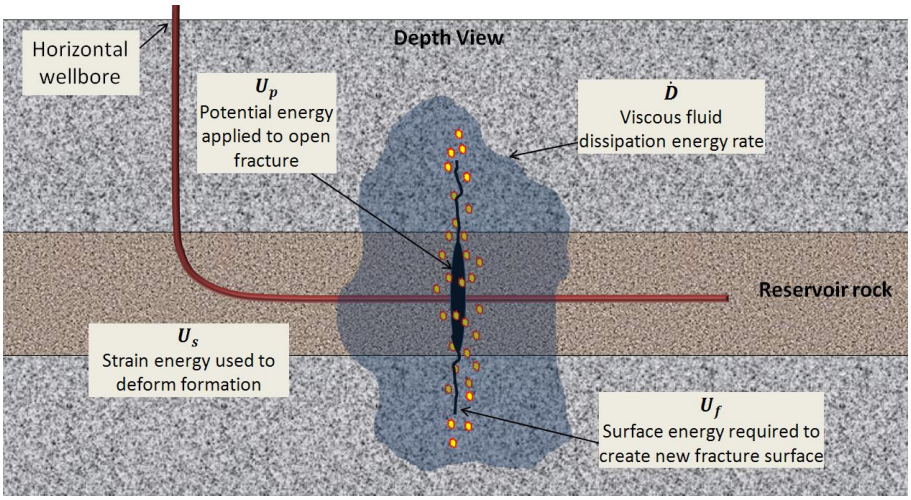

Figure 1: Cartoon of different energy components during a tensile (Mode I) hydraulic fracture surrounded by microseismic activity indicating fracture extension in a three layered medium.

The Lagrangian formulation, adapted from Advani et al. (1990) in the absence of fluid dissipation is given by:

$$\frac{\partial U_S}{\partial Y_k} + \frac{\partial U_f}{\partial Y_k} = \frac{\partial U_P}{\partial Y_k}, \tag{2}$$

where $Y_k(t)$ $k = 1, 2, 3, ..., n$ denotes the elliptical coordinates used, with semi-principal axis of an ellipse corresponding to the half-length $(Y_1 = a)$, -height $(Y_2 = b)$ and -width $(Y_3 = c)$ of the fracture.

The energy components for the isotropic formation presented by Advani et al. (1990) are reduced to: $U_p = \frac{4}{3} P_{eff} \pi abc$, $U_f = G_{cr} \pi ab$ and $U_s = 2\frac{\mu}{3(1-\upsilon)} E(k) \pi ac^2$. The term, $P_{eff}(x,t)$, is the resultant fluid pressure defined by

$$P_{eff}(x,t) = p(x,t) - \sigma_{\min}, \tag{3}$$

where $p(x,t)$ is the fluid pressure inside the crack, assumed to be uniformly distributed within the crack, t is injection time and $\sigma_{\min}$ is the minimum principle horizontal in-situ stress. The closure pressure, determined by conducting a fracture injection test, is assumed to be the minimum in-situ stress. Shear modulus and Poisson's ratio are given by μ and ν respectively and derived from logs. $E(k)$ is the complete elliptic integral of the second kind with its argument defined as $k = \sqrt{1 - \frac{b^2}{a^2}}$ (Advani et al. 1990). The critical energy release rate, G_{cr}, introduced by Irwin (1957), represents the work required to produce a unit increase in crack area. This can be written in terms of the critical stress intensity factor, K_{IC}, a relationship described by Irwin (1957),

$$G_{cr} = K_{IC}\left[\frac{\sqrt{1-\nu^2}}{\mathrm{E}}\right]. \tag{4}$$

For the symmetric three-layered case, the simplified equations are expanded on and are used to construct a system of non-linear differential equations with unknown variables $a(t)$, $b(t)$, $c(t)$ and $P_o(t)$ (Advani, 1990). Three of these equations (e.g. f_1, f_2, f_3) sum each energy term and take the derivative of each with respect to one of the quantities $a(t)$, $b(t)$ and $c(t)$. This is intended to measure the rate of change of each energy component in each direction of fracture growth. The fourth equation, corresponding to mass conservation accounting for fluid pumped (qt), leakoff volume ($\frac{2\pi abv_\eta C_T}{\sqrt{t}}$) adapted from Nolte (1984) and the fracture volume (πabc) adapted from Shlyapobersky (1985) for an elliptical crack is given by:

$$f_4 = 0 = \frac{4\pi abc}{3} + \frac{2\pi abv_\eta C_T}{\sqrt{t}} - qt \tag{5}$$

Here q is the variable fluid flow rate and, v_η is a constant ($\frac{4}{3} \le v_\eta \le \frac{\pi}{2}$) that is dependent on the total fluid loss coefficient C_T.

The four equations, f_1, f_2, f_3 and f_4 are simultaneously satisfied by a numerical scheme at each time step, $t + \Delta t$ and used to solve for $a(t)$, $b(t)$, $c(t)$ and $P_o(t)$.

Numerical Example

A single fracture treatment was used to evaluate the model results. The half-length, -height and –width were solved for and compared to the actual geometry inferred by a representative microseismic map. The input parameters required for model simulation are: payzone thickness (h), elastic moduli given as ν, E, $\mu_{payzone}$, $\mu_{barrier}$, barrier in-stress contrast ($\Delta\sigma_{\min}$) and G_{cr} along with its change in barrier layer (ΔG_{cr}). The payzone thickness was assumed to be 120m, the payzone and barrier elastic moduli,

were assumed and supplied by the operator and a small value for $\Delta\sigma_{\min}$ was used. The variable adjusted for was G_{cr}, all other parameters were kept constant for this example. Figure 2 shows the input microseismic map in depth view, overlain by the elliptical fracture simulations at different time steps. Example one in the left plot in Figure 2 assumes a low value of $G_{cr1} = 2.26x10^{-5}$ MPa-m and $\Delta G_{cr1} = 0.25G_{cr1}$ MPa-m, whereas example two in the right plot assumes a large value of $G_{cr2} = 30G_{cr1}$ MPa-m and $\Delta G_{cr2} = 0.25G_{cr2}$ MPa-m. Equation (4) was used to convert K_{IC} into G_{CR}. Typical K_{IC} values for shale formations under low confining pressures are provided in the paper by Eekelen (1982). However, Eekelen (1982) also notes that under downhole conditions these values can be higher.

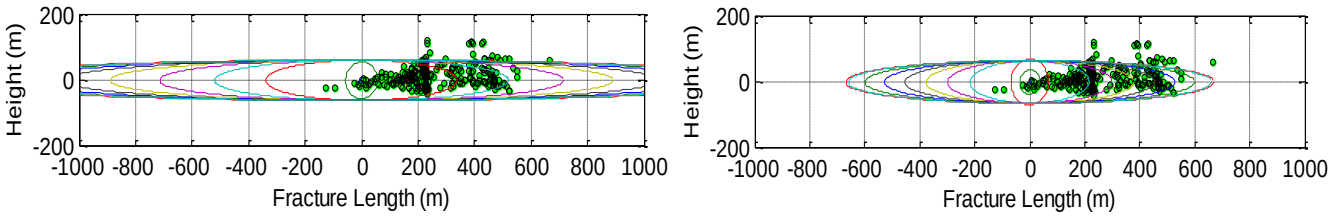

Figure 2: Microseismic image overlain with the model geometry using a small G_{cr1} (left plot) and large G_{cr2} (right plot).

A value for $\Delta\sigma$ was assumed to be 1MPa. This value was determined to be sufficient to keep the fracture contained within the payzone with little height growth once the fracture grew into the over and underlying layers. Since the elastic moduli were kept constant in both scenarios, the effects of G_{cr} on fracture geometry were mostly examined here. Given a small G_{cr}, the lateral extension is much greater than with a low G_{cr} (Figure 2). The simulations using a large G_{cr} provided a better match with the microseismic data which in Figure 1 only shows total fracture height and length. For simplicity, the microseismic event locations were assumed to have no error and be symmetric about the fracture initiation point (i.e. perforations at wellbore). A possible cause of the asymmetry in the microseismic image could be viewing bias due to placement of the geophone array in proximity to the hydraulic fracture location.

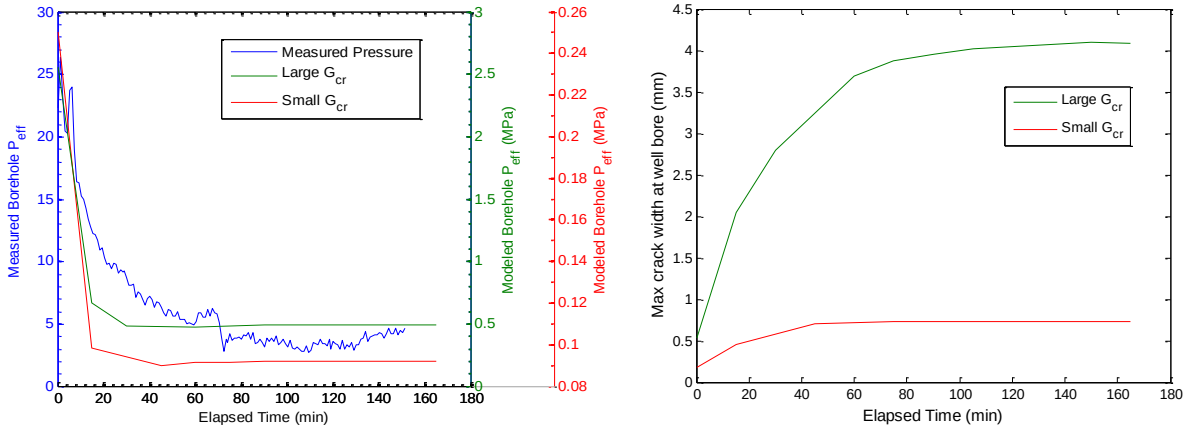

Figure 3: Profile of measured effective pressure from treatment data and modeled data (left plot) and fracture maximum fracture width at wellbore (right plot) for a large and small G_{cr}.

Figure 3 shows the result of pressure (left plot) as a function of injection time. When comparing the effective pressure profile as a result of large G_{cr} versus small G_{cr}, it can be seen that as G_{cr} increases the effective pressure profile of the fracture increases. Both the P_{eff} profile as a result of small and large

G_{cr} are much lower than the actual P_{eff}. This phenomenon requires further investigation because there are many assumptions and energy considerations that may or may not be accounted for that could explain the difference in both pressure profiles. However, all pressure curves plotted in Figure 3 consistently show exponential decay as the fracture propagates with time.

The right plot in Figure 3 shows the fracture width propagation with time as G_{cr} increases, the fracture width subsequently increases, likewise as G_{cr} is decreased, the maximum width also decreases. Width is a nearly impossible to measure directly from microseismic and therefore is often solved for analytically or numerically. In this case, it was only solved for numerically, but no other computations were available for comparison.

Assumed values for K_{IC} and consequently for G_{cr} was developed for homogenous bonded materials, not for materials such as sands or jointed rock (M. Dusseault, pers. comm., 2012). Therefore, the effects of G_{cr} on fracture evolution based on modeled results need further investigation, especially for naturally fractured formations such as shales.

Conclusions

A numerical algorithm has been developed to evaluate the effect of different reservoir parameters on fracture geometry using energy considerations. Using representative microseismic and injection data for constraints, our preliminary results show the influence that different input parameters and their response have on fracture propagation.

To demonstrate the validity of the modeling technique, a three layered symmetric model, with in-situ stress and elastic moduli contrast containing an evolving elliptical fracture, was compared to a hydraulic fracture program conducted in the field. As an example, the effect of critical energy release rate on the fracture extension was studied. Our results show that a match between real data and model data can be achieved upon optimum parameter selection. Evaluation of modulus and in-situ stress contrasts, incorporation of dissipation along with other advances is currently in progress. However, by showing a numerical example, we conclude that the use of pertinent energies, appropriate parameterization and the use of microseismic data for validation, this model can serve as an effective tool for fracture design and field planning of unconventional reservoirs.

Acknowledgements

We gratefully acknowledge financial support for this project from the Microseismic Industry Consortium and the Natural Sciences and Engineering Research Council of Canada. We are grateful to Nexen Inc. for providing the data for this study and to Hassan Khaniani for valuable discussions.

References

Advani, S.H. , Lee, T.S., and Moon, H., 1990, Energy considerations associated with the mechanics of hydraulic fracture: SPE 21296.

Irwin, G. R. 1957. Analysis of stress and strains near the end of a crack traversing a plate. J. appl. Mech. 361-364.

Warpinski, N.R. & Teufel, L. W., 1987. Influence of Geologic Discontinuities on Hydraulic Fracture Propagation. JPT: Feb. issue, 209-220.

Shlyapobersky, J. 1985. Energy analysis of hydraulic fracturing. 26th US Symposium on Rock Mechanics. Rapid City, SD. June issue 26-28

Biot, M.A., Masse, L. & Medlin, W.L. A two-dimentional theory of fracture propagation. SPEPE(Jan. 1986) 17-30.

Perkins T.K. and Krech W.W. The energy balance concept of hydraulic fracturing. Soc. Pet. Eng. J, 1986, vol.243, pp.1-12.

Lee, T.S., Advani, S. H. Avasthi, J.M. , 1991, Characteristic-time concept in hydraulic fracture configuration evolution and optimization.: SPEPE 23552.

Van Eekelen H.A. 1982. Hydraulic fracture geometry: fracture containment in layered formations. Soc. Pet. Eng. J. vol.22, pp.341-347

EPA. June 2004. Chapter 4: Hydraulic fracturing fluids

M. Dusseault, pers. comm., 2012